Vol 13 No 7, July 2004
1009-1963/2004/13(07)/1156-07

Chinese Physics

© 2004 Chin. Phys. Soc.
and IOP Publishing Ltd

Infrared-to-green upconversion luminescence and mechanism of Ho^{3+}, Nd^{3+} and Yb^{3+} ions in oxyfluoride glass ceramics*

Zhang Jun-Jie(张军杰)[a)†], Kawamoto Yoji[b)], and Dai Shi-Xun(戴世勋)[a)],

[a)] *Shanghai Institute of Optics and Fine Mechanics, Chinese Academy of Sciences, Shanghai* 201800, *China*

[b)] *Department of Chemistry, Faculty of Science, Kobe University, Rokkodai, Nada, Kobe* 657-8501, *Japan*

(Received 21 November 2003; revised manuscript received 16 January 2004)

New oxyfluoride glasses and glass ceramics co-doped with Nd^{3+}, Yb^{3+} and Ho^{3+} were prepared. The upconversion of infrared radiation into green fluorescence has been studied for Nd^{3+}, Yb^{3+} and Ho^{3+} in the transparent oxyfluoride glass ceramics. At room temperature very strong green upconversion luminescence due to the Ho^{3+}: $(^5F_4, {}^5S_2) \rightarrow {}^5I_8$ transition under 800 nm excitation was observed in the glass ceramics. The intensity of the green upconversion luminescence in a 1mol% YbF_3-containing glass ceramic was found to be about 120 times stronger than that in the precursor oxyfluoride glass. The reason for the highly efficient Ho^{3+} upconversion luminescence in the oxyfluoride glass ceramics is discussed. The upconversion mechanism is also investigated.

Keywords: upconversion, mechanism, oxyfluoride glass ceramics
PACC: 7820, 8160F, 8160D

1. Introduction

There is a great interest in glass ceramics for the conversion of infrared radiation into visible light. This phenomenon is useful for the detection of infrared radiation by changing the light to a spectral region where detectors have higher efficiency. It has been shown that infrared light of about 1μm can be efficiently converted into visible light by some phosphors activated by Er^{3+}, Ho^{3+} or Tm^{3+} etc. and sensitized by Yb^{3+}.[1–3]

This infrared-to-visible conversion phenomenon is caused by the accumulation of infrared photon energy to the activator rare-earth ions. Its mechanism involves various elementary processes such as energy transfer and relaxation transition, and is dominated by the nature of the electron–phonon interaction as well as of the ion–ion interaction. This phenomenon is not only interesting from the basic point of view, but is also very important from the practical viewpoint of solid state electronics.

The infrared-to-green or -blue upconversion luminescence has been extensively investigated in a variety of rare-earth-doped crystalline and vitreous materials. Recently, rare-earth-containing oxyfluoride glass ceramics have aroused interest in connection with applications in upconversion and light amplification.[4–7] In such glass ceramics, rare-earth elements are preferentially incorporated into crystalline phases with small phonon energies below $500cm^{-1}$, where their active optical properties may be brought to optimum conditions.[4]

Rare-earth-doped oxyfluoride glass ceramics were reported in the 1970s.[8] These glass ceramics are produced by melting of oxyfluoride glasses followed by heat treatments above the glass transition temperatures. Such heat treatments give secondary phases consisting of fluorite-type crystals in which doped rare-earth ions are selectively partitioned.[5,6] The size of the crystalline domains can be sufficiently small so as not to cause excess light scattering. Consequently, the obtained glass ceramics are transparent to the naked eye. The great advantages of this approach are the following: (1) doped rare-earth ions

*Project supported by the National Natural Science Foundation of China (Grant No 60207006), and by the Optical Science and Technology of Shanghai (Grant No 022261046).

†To whom correspondence should be addressed. E-mail: jjzhang@siom.ac.cn

are confined in crystalline environment of low phonon energies; consequently, excited-state lifetimes and optical absorption cross-sections of the doped rare-earth ions become substantially larger in them than in vitreous environments; (2) the glass host matrices are based on silicates with mechanically and chemically desirable characteristics.

In this paper the upconversion of infrared radiation into green luminescence and the mechanism of the Ho^{3+} upconversion luminescence in Nd^{3+}-Yb^{3+}-Ho^{3+} co-doped oxyfluoride glass ceramics are reported, possibly for the first time in the literature.

2. Experimental procedure

Glasses were prepared using a conventional melt-quenching method. High purity SiO_2, Al_2O_3, PbF_2, CdF_2, NdF_3, HoF_3 and YbF_3 were used as the starting materials. Compositions chosen in the present study are $30SiO_2{\cdot}15AlO_{1.5}{\cdot}28PbF_2{\cdot}22CdF_2{\cdot}$ $(4.8{-}x)$ $GdF_3{\cdot}0.1NdF_3{\cdot}0.1HoF_3 \cdot xYbF_3$ (x=0, 0.1, 0.2, 0.5, 1, 2, 3, 4 and 4.8) in mol%. Accurately weighed 5-gram batches were thoroughly mixed and moved into Pt crucibles. The batches were melted at 950°C for 15min in an electric furnace with very rapid heating-rates in an air atmosphere. The melts were cast into preheated brass moulds. The obtained glasses were annealed at the respective glass transition temperatures determined by differential thermal analysis (DTA).

The thermal properties of the glasses were measured by DTA. The measurements were performed with a Rigaku Thermo Plus TG-DTA TG8110 apparatus at a heating rate of 10 $K{\cdot}min^{-1}$ in an Ar atmosphere.

All the prepared glasses were heat-treated at the same temperature of 450°C for 0.5h. In order to confirm crystal precipitation, x-ray diffraction measurements were carried out on the precursor glasses and the heat-treated glasses with a Rigaku RINT 2100 x-ray diffractometer using Cu Kα radiation.

Upconversion luminescence spectra of Ho^{3+} under 800nm excitation were measured in the wavelength range of 400–700nm with a Hitachi F-3010 fluorescence spectrophotometer. A Sony SLD303-XT AlGaAs laser (maximum output power 150mW) was used as an excitation source. Specimens of the size of $5.0{\times}5.0{\times}1.2mm^3$ with optically flat surfaces were used in the measurements.

Optical absorption spectra in the wavenumber range of 3500–30000cm^{-1} were measured with a Shimadzu UV-2200 spectrophotometer.

Fluorescence lifetimes of the Ho^{3+}: ($^5F_4$, $^5S_2$) levels were measured with a PTI-210SK spectrophotometer.

All the spectral measurements were performed at ambient temperature.

3. Results

Figure 1 shows the DTA curves of the $30SiO_2{\cdot}$ $15AlO_{1.5}{\cdot}28PbF_2{\cdot}$ $22CdF_2{\cdot}$ $(4.8{-}x)$ $GdF_3{\cdot}$ $0.1NdF_3$ $\cdot$ $0.1HoF_3{\cdot}$ $xYbF_3$ (x=0, 1 and 4.8) glasses where T_g and T_x indicate the glass transition temperatures and the first crystallization temperatures, respectively. The T_g and T_x values increased with increasing YbF_3 concentration, though very slightly.

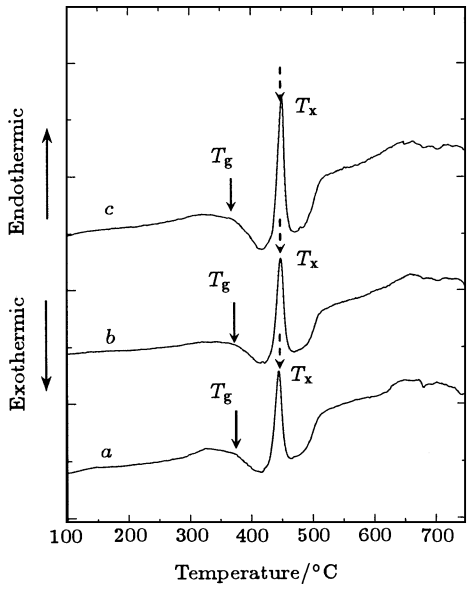


Fig.1. DTA curves of $30SiO_2{\cdot}15AlO_{1.5}{\cdot}28PbF_2{\cdot}22CdF_2{\cdot}$ $(4.8{-}x)$ $GdF_3{\cdot}0.1NdF_3{\cdot}0.1HoF_3{\cdot}x$ YbF_3 glasses (curve a, x=0; curve b, x=1 and curve c, x=4.8).

Figure 2 shows the representative x-ray diffraction patterns of the $30SiO_2{\cdot}15AlO_{1.5}{\cdot}28PbF_2{\cdot}22CdF_2{\cdot}$ $3.8GdF_3{\cdot}0.1NdF_3{\cdot}0.1HoF_3{\cdot}1YbF_3$ glasses before and after heat treatment. A broad halo pattern characteristic of glass structure was observed for the samples before heat treatment, whereas several sharp diffraction peaks characteristic of crystalline structure were clearly observed for the samples after heat treatment, indicating that crystals were successfully precipitated during heat treatment. All the glass ceramics obtained after heat treatment were transparent. A comparison of the XRD pattern of crystals precipitated in the glass ceramics with those of β-PbF_2 and CdF_2 crystals with a fluorite-type structure is shown in Fig.2. As can be seen from this figure the peak positions in the glass ceramics are located at slightly higher angles respective

to the PbF_2 crystal patterns and at lower angles respective to the CdF_2 crystalline patterns. Therefore, it is reasonable to consider that the crystalline phase in the present glass ceramics has a mixed fluorite-type structure of PbF_2 and CdF_2, i.e. $Pb_xCd_{1-x}F_2$. By using the following Debye–Scherrer equation:[9]

$$D_{hkl} = \frac{0.9\lambda \times 57.3}{\beta_{1/2} \cos\theta}, \quad (1)$$

where λ is the wavelength of the x-rays, $\beta_{1/2}$ is the half-maximum line breadth in radians, and θ is the diffraction angle, the size of the crystalline precipitates was evaluated to be approximately 16.3nm in diameter.

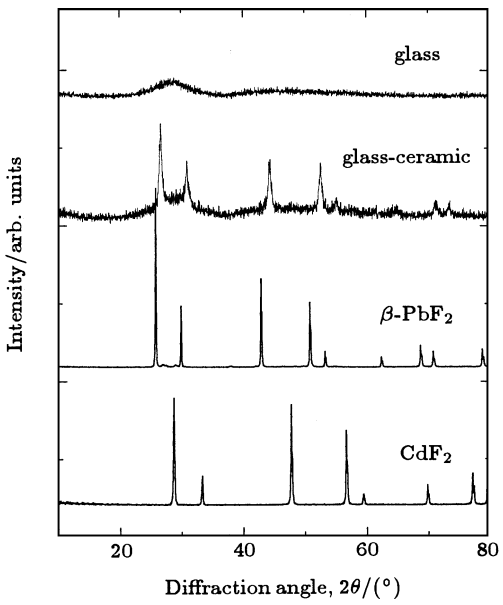


Fig.2. Powder XRD patterns of $30SiO_2{\cdot}15AlO_{1.5}{\cdot}28PbF_2{\cdot}22CdF_2{\cdot}3.8GdF_3{\cdot}0.1NdF_3{\cdot}0.1HoF_3{\cdot}1YbF_3$ glass and glass ceramic, together with those of β-PbF_2 and CdF_2 crystals.

In Fig.3, upconversion luminescence spectra of Ho^{3+} in the $30SiO_2{\cdot}15AlO_{1.5}{\cdot}28PbF_2{\cdot}22CdF_2{\cdot}3.8GdF_3{\cdot}0.1NdF_3{\cdot}0.1HoF_3{\cdot}1YbF_3$ glass under 800nm excitation before and after heat treatment are presented. Three emission bands centred around 490 (blue), 545 (green) and 650nm (red), which correspond to the Ho^{3+}: ($^5F_3 \rightarrow {}^5I_8$), ($^5F_4$, $^5S_2 \rightarrow {}^5I_8$) and ($^5F_5 \rightarrow {}^5I_8$) transitions, respectively, were observed in the $30SiO_2{\cdot}15AlO_{1.5}{\cdot}28PbF_2{\cdot}22CdF_2{\cdot}(4.8{-}x)GdF_3{\cdot}0.1NdF_3{\cdot}0.1HoF_3{\cdot}xYbF_3$ glasses after heat treatment (glass ceramics). In the case of the glasses before heat treatment (precursor glasses), however, only green and red emission bands were observed and no blue emission band was detected. It is worth noting that, in a 1 mol% YbF_3-containing glass, the intensity of 545nm luminescence after heat treatment is about 120 times stronger than that before heat treatment, and is about 40 times stronger than that in the glass with 3 mol% YbF_3 concentration. As shown in Fig.4, it was found that the intensity ratios of green luminescence to red luminescence, I_{545}/I_{660}, greatly change with the YbF_3 concentration in the glass ceramics, whereas the ratios in the glasses before heat treatment are almost independent of YbF_3 concentration. Figure 5 shows the YbF_3 concentration dependence of Ho^{3+} green upconversion luminescence intensities in the $30SiO_2{\cdot}15AlO_{1.5}{\cdot}28PbF_2{\cdot}22CdF_2{\cdot}(4.8{-}x)GdF_3{\cdot}0.1NdF_3{\cdot}0.1HoF_3{\cdot}xYbF_3$ glasses and glass ceramics (x=0, 0.1, 0.2, 0.5, 1, 2, 3, 4 and 4.8). The intensity of the 545nm green upconversion luminescence in the glasses gradually increases with increasing YbF_3 concentration, reaching the maximum value at approximately 3mol % YbF_3 and then very slightly decreases with further increase of YbF_3 content. On the other hand, the intensity of the 545nm upconversion luminescence in glass ceramics steeply increases with increasing YbF_3 concentration, reaching the maximum value at approximately 1mol% YbF_3 and then greatly decreases with increasing YbF_3 concentration.

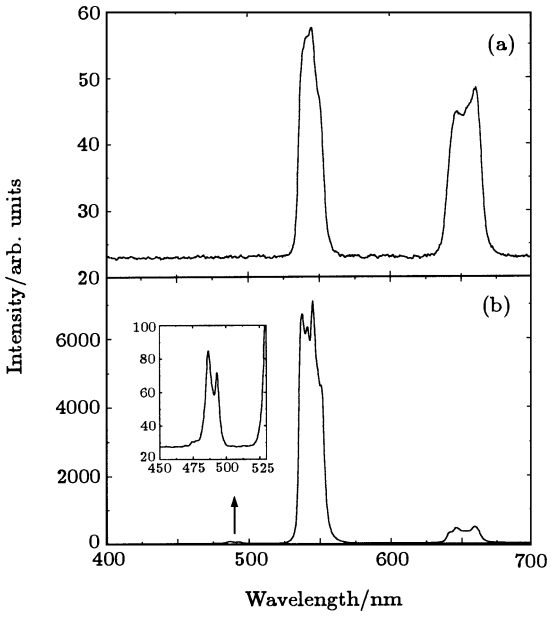


Fig.3. Upconversion luminescence spectra under 800nm excitation in $30SiO_2{\cdot}15AlO_{1.5}{\cdot}28PbF_2{\cdot}22CdF_2{\cdot}3.8GdF_3{\cdot}0.1NdF_3{\cdot}0.1HoF_3{\cdot}1YbF_3$ glasses (a) before and (b) after heat treatment at 450°C for 30min.

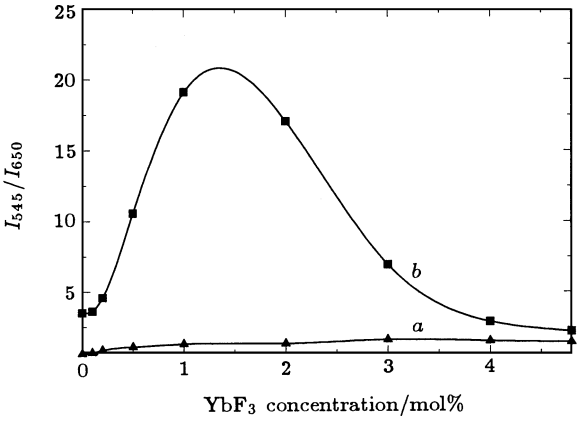


Fig.4. YbF_3 concentration dependence of ratio of green luminescence to red luminescence, I_{545}/I_{650}, in oxyfluoride glasses (curve *a*) and glass ceramics (curve *b*) under 800nm excitation.

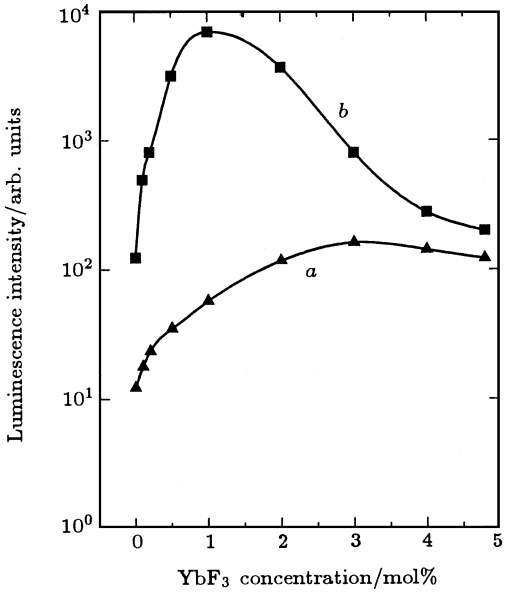


Fig.5. YbF_3 concentration dependence of Ho^{3+} green upconversion luminescence intensity in oxyfluoride glasses (curve *a*) and glass ceramics (curve *b*) under 800 nm excitation.

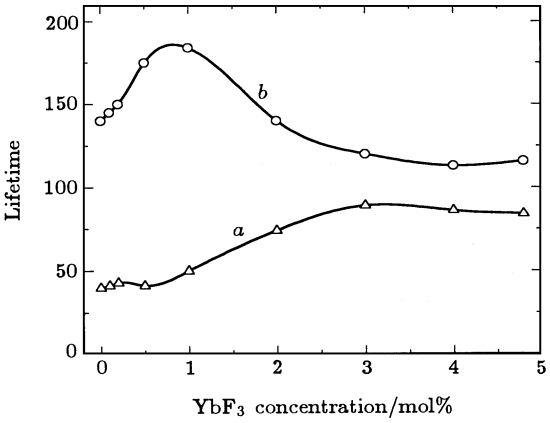


Fig.6. YbF_3 concentration dependence of lifetime of Ho^{3+}fluorescence of 545nm in oxyfluoride glasses (curve *a*) and glass ceramics (curve *b*) under 537nm excitation.

4. Discussion

4.1. Contribution of ligand field change around rare-earth ions to Ho^{3+} upconversion luminescence efficiency

According to the Miyakawa–Dexter theory,[10] a non-radiative decay rate due to a multiphonon relaxation process is governed by both phonon energy and electron–phonon coupling strength. The larger the phonon energy and/or the electron–phonon coupling strength, the larger the non-radiative decay rate. That is to say, a decrease in phonon energy and /or electron–phonon coupling strength increases the lifetimes and quantum efficiencies of excited levels and consequently increases the emission intensity of upconversion luminescence. As a result, a matrix of low phonon energy, e.g. fluoride matrix, is generally of benefit to frequency upconversion.

In oxyfluoride glasses, rare-earth ions, e.g. Ho^{3+}, are readily coupled to the non-bridging oxygen on the strong O–Si and/or O–Al bonds.[3] Such a coupling causes an increase in non-radiative decay rate due to multiphonon relaxation and greatly reduces the lifetimes of levels involved in the upconversion processes. Like most oxide glasses, therefore, oxyfluoride glasses are also not efficient for upconversion. On the other hand, rare-earth ions in the present oxyfluoride glass ceramics are incorporated into a fluorite-type solid solution so that the coordination environments around rare-earth ions leads to low phonon energy.

Figure 6 shows a comparison of the YbF_3 concentration dependence of the lifetime of Ho^{3+}: ($^5F_4$, $^5S_2$) $\rightarrow$ $^5I_8$ fluorescence of 545nm in the $30SiO_2 \cdot 15AlO_{1.5} \cdot 28PbF_2 \cdot 22CdF_2 \cdot (4.8-x)\,GdF_3 \cdot 0.1NdF_3 \cdot 0.1HoF_3 \cdot x YbF_3$ (x=0, 0.2, 0.5 1.0, 2.0, 3.0, 4.0 and 4.8) glasses and glass ceramics under 537nm excitation. In the present lifetime measurements, 4f electrons are directly excited to Ho^{3+}: ($^5F_4$, $^5S_2$) level. The lifetimes after heat treatment greatly increase compared with those before heat treatment. Especially, for the 1 mol% YbF_3-containing glass and glass ceramic the respective lifetimes are 50 and 184 μs. This result also proves that rare-earth ions, i.e. Nd^{3+}, Yb^{3+} and Ho^{3+}, are incorporated into a fluorite-type solid solution phase.

In such a case, rare-earth ions would be shielded from the direct coupling with the non-bridging oxygen of O–Si and/or O–Al. Consequently, an upconversion efficiency as high as that in pure fluoride glasses or crystals becomes achievable. The SiO_2 and $AlO_{1.5}$ (Al_2O_3) components behave as glass matrices embedding a fluorite-type nanocrystal including Nd^{3+}, Yb^{3+} and Ho^{3+}. This is the reason why the Ho^{3+} upconversion luminescence is hardly observed in the glasses before heat treatment (precursor glasses), but it is strongly observed in the glass ceramics after heat treatment (glass ceramics). According to the Miyakawa–Dexter theory [10] the multiphonon decay rate, W_p, is expressed by

$$W_p = W_0 \exp(-\alpha \Delta E/h\omega), \qquad (2)$$

where W_p is the multiphonon decay rate, ΔE is the energy gap to the next lower level and $h\omega$ is the phonon energy. Figure 7 presents the optical absorption spectrum of Ho^{3+} in the $30SiO_2 \cdot 15AlO_{1.5} \cdot 28PbF_2 \cdot 22CdF_2 \cdot 4GdF_3 \cdot 1HoF_3$ glass. The energy gap between the $^5F_2$, $^3K_8$ levels and the next lower level $^5F_3$ is about $560cm^{-1}$. This energy gap is very narrow and the former level is very sensitive to a change of ligand field. Kawamoto *et al*[11] have found that rare-earth ions in the $50SiO_2 \cdot 50PbF_2 \cdot xErF_3$ glasses (x=4 and 5) are strongly coupled to a phonon mode of $930cm^{-1}$, but those in the glass ceramics (crystalline phase: a β-PbF_2 solid solution) are strongly coupled to a phonon mode of $230cm^{-1}$. Since non-radiative decay is due to multiphonon relaxation, it is understandable that blue (490nm) upconversion luminescence is not observed in oxyfluoride glass, but is observed in oxyfluoride glass ceramics.

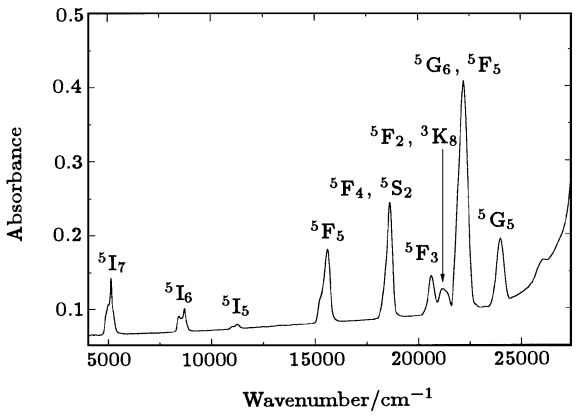


Fig.7. Optical absorption spectrum of Ho^{3+} in $30SiO_2 \cdot 15AlO_{1.5} \cdot 28PbF_2 \cdot 22CdF_2 \cdot 4GdF_3 \cdot 1HoF_3$ glass.

4.2. Dependence of Ho^{3+} upconversion luminescence upon Yb^{3+} concentration

It is known that the probability of energy transfer due to multi-polar interactions relates to the distance R between a sensitizer and an acceptor. According to the Dexter theory [12] the energy transfer probability in dipole–dipole interaction is proportional to R^{-6}. As described in Ref.[10], the Ho^{3+} upconversion luminescence decreases with an increase in the Nd^{3+} and/or Ho^{3+} concentrations. This has been considered to be due to the self-quenching of Nd^{3+} and/or Ho^{3+} in their high concentration regions. On the other hand, Yb^{3+} ions have only one excited state above the ground state. A Yb^{3+} donor ion in the excited state transfers all of its excitation energy to a Yb^{3+} acceptor ion in the ground state. This process can be repeated many times, resulting in the energy migration through the material. The energy migration would continue until some other mechanism depletes the excited state. In the case of Nd^{3+}-Yb^{3+}-Ho^{3+} co-doped glasses, Yb^{3+} ions play a role as energy transfer bridging ions. In this case, the distance between Nd^{3+} ions and Ho^{3+} ions becomes contracted with the Yb^{3+} addition and consequently the efficiency of energy transfer from Nd^{3+} ions to Ho^{3+} ions becomes high, and Ho^{3+} upconversion luminescence becomes stronger. As shown in Fig.5, however, the Ho^{3+} green upconversion luminescence intensity exhibits a maximum value, depending on Yb^{3+} concentration in the glasses and the glass ceramics, respectively, and the respective maximum values are different. A similar tendency is observed in the lifetime measurements of Ho^{3+}: ($^5F_4$, $^5S_2$) levels, as shown in Fig.6. In glasses with high rare-earth concentrations, in contrast, energy back-transfer cannot be neglected. Here, it is considered that the energy back-transfer occurs from Ho^{3+} to Yb^{3+} in the high YbF_3 concentration regions: energies on the Ho^{3+}: ($^5F_4$, $^5S_2$) levels are back-transferred to Yb^{3+} by the cross-relaxation of [Ho^{3+}: ($^5F_4$, $^5S_2$) $\rightarrow ^5I_6$]; [Yb^{3+}: $^2F_{5/2} \leftarrow ^2F_{7/2}$]. Since the Nd^{3+}, Yb^{3+} and Ho^{3+} ions are concentrated into fluorite-type nanocrystals, the distances between Ho^{3+} ions and Yb^{3+} ions become closer. This may be the reason why the maximum intensity of Ho^{3+} upconversion luminescence appears at different YbF_3 concentration values in the glasses and the glass ceramics.

As can be seen from Fig.4, it is notable that the intensity ratios of green luminescence to red lumines-

cence, I_{545}/I_{650}, in the glasses and the glass ceramics are different. Even in similar environment in glass ceramics, the I_{545}/I_{650} ratio greatly changes with YbF_3 concentration. As described in Sec.4.1, energy loss by non-radiative relaxation becomes smaller with the change in ligand field around a rare-earth ion. The optical absorption cross-section of Yb^{3+} becomes larger in the glass ceramics than in the glasses. This result leads to high efficiency in energy transfer from Nd^{3+} ions to Ho^{3+} ions via Yb^{3+} ions in the glass ceramics. Therefore, the intensity ratios of green luminescence to red luminescence greatly change before and after the fluorite-type nanocrystal precipitation. The distances between Ho^{3+} ions and Yb^{3+} ions become closer in the glass ceramics, with vigorous energy back-transfer from Ho^{3+} to Yb^{3+} due to [Ho^{3+}: ($^5F_4$, $^5S_2$) $\rightarrow{}^5I_6$]; the [Yb^{3+}: $^2F_{5/2}$ $\leftarrow{}^2F_{7/2}$] transition greatly affects the efficiency of green upconversion luminescence; the YbF_3 concentration affects the efficiency of green upconversion luminescence, and hardly affects the efficiency of red upconversion luminescence. So it is considered that the upconversion mechanisms for green (545nm) and red (650nm) are different. This results in the increase of I_{545}/I_{650} ratio in the low YbF_3 concentration regions, and decrease of I_{545}/I_{650} ratio in the high YbF_3 concentration regions.

4.3. Upconversion luminescence mechanism in Nd^{3+}-Yb^{3+}-Ho^{3+} co-doped glass and glass ceramics

The present authors and co-workers have already studied the Ho^{3+} upconversion luminescence mechanism in Nd^{3+}-Ho^{3+} and Nd^{3+}-Yb^{3+}-Ho^{3+} co-doped fluoride glasses.[13,14] Based on the result, an upconversion mechanism in the present Nd^{3+}-Yb^{3+}-Ho^{3+} co-doped oxyfluoride glass ceramics under 800nm excitation is proposed, as depicted in Fig.8. In the first step, Nd^{3+} ions are excited by 800nm radiation which corresponds to the Nd^{3+}: ($^4F_{5/2}$, $^2H_{9/2}$) $\leftarrow{}^4I_{9/2}$ transitions. The ($^4F_{5/2}$, $^2H_{9/2}$) excited states relax quickly to the next-lower $^4F_{3/2}$ state by a multi-phonon relaxation and then an energy transfer between Nd^{3+} ions and Yb^{3+} ions, [Nd^{3+}: $^4F_{3/2}$ $\rightarrow{}^4I_{9/2}$ and/or $^4I_{11/2}$; Yb^{3+}: $^2F_{5/2}$ $\leftarrow{}^2F_{7/2}$], occurs with considerably high efficiencies. At the same time, Ho^{3+} ions absorb 800nm photons, provoking the Ho^{3+}: $^5I_4$ $\leftarrow{}^5I_8$ transition, and then the $^5I_5$ level is populated through a non-radiative relaxation process. Subsequently the energies on the Yb^{3+} ions are transferred to the Ho^{3+} ions which are on the $^5I_5$ level, resulting in the Ho^{3+}: ($^5F_2$, $^3K_8$) $\leftarrow{}^5I_5$ excitation. Then the 4f electrons non-radiatively relax from the ($^5F_2$, $^3K_8$) states to the $^5F_3$ or ($^5F_4$, $^5S_2$) states by multi-phonon relaxation. Finally, these 4f electrons on these states radiatively relax to the $^5I_8$ ground state, giving the blue (490nm) and green (545nm) upconversion luminescences.

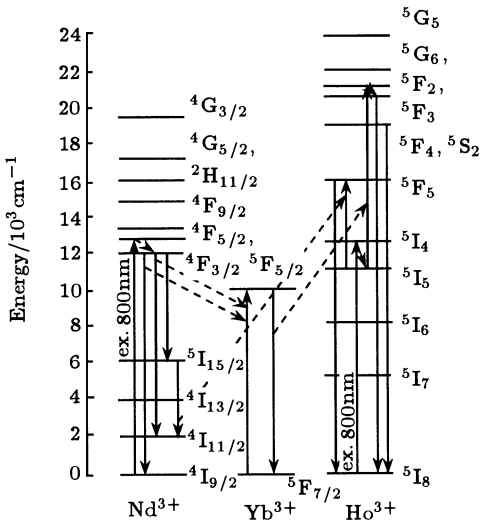


Fig.8. Schematic upconversion mechanism in $30SiO_2$· $15AlO_{1.5}$· $28PbF_2$· $22CdF_2$· $(4.8–x)$ GdF_3· $0.1NdF_3$· $0.1HoF_3$· $x YbF_3$ glass ceramics under 800nm excitation.

On the other hand, because the change of YbF_3 concentration hardly effects the efficiency of red upconversion luminescence, so the upconversion mechanism for red (650nm) emission may be proposed as follows: The energy transfer from Nd^{3+} to Ho^{3+} is due to the cross-relaxation of the $^4I_{15/2}$ $\rightarrow{}^4I_{11/2}$ transition instead of the $^4F_{3/2}$ $\rightarrow{}^4I_{11/2}$ transition. That is, the Ho^{3+}: 4f electrons of the $^5I_5$ state absorb a photon due to Nd^{3+}:$^4I_{15/2}$ $\rightarrow{}^4I_{11/2}$ transition, and are excited to the $^5F_5$ state, then radiatively relax from the $^5F_5$ state to the $^5I_8$ ground state, giving red (650nm) upconversion luminescence.

5. Conclusion

In summary, we prepared Nd^{3+}-Yb^{3+}-Ho^{3+} co-doped $30SiO_2$· $15AlO_{1.5}$· $28PbF_2$· $22CdF_2$· $(4.8–x)$ GdF_3· $0.1NdF_3$· $0.1HoF_3$· $x YbF_3$ oxyfluoride glasses and glass ceramics. The experimental results indicate that the heat treatment of the Nd^{3+}-Yb^{3+}-Ho^{3+} co-doped oxyfluoride glasses at 450°C for 0.5h gave transparent glass ceramics in which fluorite-type nanocrystals with a diameter of about 16.3nm are dispersed in the glass matrix. Compared to the glasses, the glass ceramics showed green upconversion luminescence of Ho^{3+} with very high efficiency under 800nm excita-

tion. The intensity of green upconversion luminescence in a 1mol% YbF_3-containing glass ceramic was about 120 times stronger than that in the glass. The key reason is due to a difference in the co-ordination environments around the Nd^{3+}-Yb^{3+}-Ho^{3+} ions in the oxyfluoride glasses before and after heat-treatment. It is considered that the Nd^{3+}-Yb^{3+}-Ho^{3+} co-doped oxyfluoride glass ceramics obtained in this study gives a good promise for using it as a green solid-state laser medium.

References

[1] Hewes R A and Sarver J F 1969 *Phys. Rev.* **182** 427

[2] Guggenheim H J and Johnson L F 1966 *Appl. Phys. Lett.* **15** 51

[3] Xiao S, Yang X and Liu Z 2002 *Chin. Phys.* **11** 188

[4] Quimby R S, Tick P A and Borrelli N F and Cornelius L K 1998 *J. Appl. Phys.* **83** 1649

[5] Auzel F, Lipinska-Kalita K E and Santa-Cruz P 1996 *Opt. Mater.* **5** 75

[6] Wang Y and Ohwaki J 1993 *Appl. Phys. Lett.* **63** 3268

[7] Tick P A, Borrelli N F, Cornelius L K and Newhouse M A 1995 *J. Appl. Phys.* **78** 11

[8] Auzel F, Pecile D and Morin D 1975 *J. Electrochem. Soc.* **122** 101

[9] Klug H P and Alexander L E 1954 *X-ray Diffraction Procedures for Polycrystalline and Amorphous Materials* (New York: Wiley) p51

[10] Miyakawa T and Dexter D L 1970 *Phys. Rev.* B **1** 2961

[11] Kawamoto Y, Kanno R and Qiu J 1998 *J. Mater. Sci.* **33** 63

[12] Dexter D L 1965 *J. Chem. Phys.* **43** 1978

[13] Qiu J, Shojiya M and Kawamoto Y 1999 *J. Appl. Phys.* **86** 909

[14] Qiu J, Shojiya M, Kanno R, Kawamoto Y and Takahashi M 1998 *J. Phys. Condens. Matter* **10** 11095